THERMAL GRADIENT EFFECTS ON THE DYNAMIC STRESSES, DEFORMATIONS AND VIBRATIONS OF ROTATING GAS TURBINE BLADES

Dr. Muhsin J. Jweeg **Dr. Adnan N. Jamel** **Kasim A. Attya**
Department of Mechanical Engineering, University of Baghdad, Baghdad, Iraq

ABSTRACT
Rotating turbine blades are the important parts in gas turbines. Hence, an accurate estimation of stresses, deformations and vibration characteristics are required in the design to avoid failure and to obtain an optimum weight and cost. Because in recent years interest in the effect of temperature on solid bodies has greatly increased, thermal effects are investigated in addition to the rotational effects.
This work presents the numerical solutions of the blade using degenerated curved shell theory. A finite element package has been developed using the degenerated curved shell element as a discretization element in order to obtain the stresses, deformations and vibration characteristics of the rotating blades. The numerical results are compared with experimental and theoretical results in the published literature and they showed good agreement.

KEY WORDS
Thermal gradient effects, dynamic stresses, vibrations, gas turbine blades

الخلاصة
تعتبر عنفة التوربين الدوارة من أهم أجزاء التوربين الغازي، لذلك فالتقييم الصحيح للأجهادات والتشوهات وخواص الأهتزازات مطلوب عند التصميم لتجنب الفشل وللحصول على الكلفة والوزن المثاليين. وبسبب الزيادة الكبيرة في أهمية تأثير درجة الحرارة في الأجسام الصلدة في السنوات الأخيرة، تم دراسة التأثيرات الحرارية إضافة إلى التأثيرات ألد ورانية. بالإضافة إلى ذلك تم أيجاد حل عددي بأستخدام نظرية القشرة المنحنية ، كذلك تم تطوير نموذج للعناصر المحددة بأستخدام عنصر القشرة المنحنية كعنصر تجزئة لحساب الأجهادات والتشوهات و خواص الأهتزازات في الريش الدوارة. وقورنت النتائج العددية مع النتائج العملية والنظرية المنشورة و أعطت نتائج مقبولة وجيدة.

INTRODUCTION
Blades are important and expensive parts of turbomachinery. A turbomachine blade can be considered as a cantilever beam, of asymmetrical cross-section, fixed at its base, and pre-twisted from the fixed end to the free end. It is usually mounted on a rotating disk at a stagger or skew angle in such a way that pre-twisting and skewing is in the same direction. The pre-twist of the blade

causes coupling in both bending directions, in addition the asymmetry of the cross-section causes coupling with the torsional motion of the blade.

The gas temperatures in modern gas turbines range between 900 °C and 1100 °C, the material temperature that the designer permits will naturally depend on the stresses present. It seldom exceeds 1000 °C, and only unstressed parts made of corrosion resistant materials may reach higher temperatures. In order to reach these higher temperatures, blade cooling will take first place because it can be realized through heat transfer calculations and proper design.

In recent years, interest in the effect of temperature on solid bodies has increased because of rapid developments in space technology, high-speed atmospheric flights, and nuclear energy applications. The purpose of this note is to study the effect of a constant thermal gradient on coupled bending-bending-torsional vibrations of pre twisted blades.

An excellent classical study on the analysis of blades and disks was presented by Carnegie Carnegie, [1957], static bending of pre-twisted cantilever blading was examined. The blading is pre-twisted linearly about the center of its cross section to a maximum angle of π/2 radians, and is considered fixed at the root. He applied calculus of variations and static equilibrium equations were derived from expressions for the total energy of blades subject to either concentrated or uniformly distributed bending loads.

Fauconneau and Marangont, [1970] investigated the effect of a constant thermal gradient on the transverse vibrational frequencies of a simply supported rectangular plate. They obtained bounds for the eigen frequencies for various width to length plate ratios as functions of a parameter related to the temperature dependence of the modulus of elasticity of the material.

Sisto and Chang, [1984] presented a finite element method of discretizing beam segments of pre-twist rotating blades. Employing the matrix displacement method, stiffness and mass properties are developed from basic mechanics of pre-twisted beam theory. By introducing the proper displacement functions, the structural stiffness matrix and the effect of rotor blade rotational motion on the stiffness matrix are obtained systematically from the potential and kinetic energy functions.

Tomar and Jain, [1984] investigated the effect of a constant thermal gradient on coupled vibrations of a beam of linearly varying semi circular cross section attached to a rotating disk. They used a method based on the frequencies corresponding to the first three modes of vibrations, and found the effect of thermal gradient on frequencies of a wedge shaped rotating beam. Later they used the same method but to study coupled bending-tortional vibrations of a pre-twist slender beam.

Omprakash and Ramamurti, [1989] carried out the steady state dynamic stress and deformation analysis of high pressure stage turbomachinery bladed disks taking into account all the geometric complexities involved and the contributions due to initial stress and membrane behavior. They used a triangular shell element with six degrees of freedom per node. Abbas and Irretier, [1989] investigated experimentally the combined effect of rotary inertia, shear deformation and flexibility on the vibration characteristics of blade turbine, and compared the experimental results with theoretical results obtained by, the finite element method and the numerical integration method.

THERMAL EFFECT

It is assumed that the blade is subjected to a steady one dimensional temperature distribution along the length, i.e., in the z-direction Tomar and Jain, [1985]:

$$T_1 = T_o(1-\bar{\zeta}) \qquad (1)$$

Where T denotes the temperature excess above the reference temperature at any point at a distance $\bar{\zeta}$=Z/L and T_o denotes the temperature excess above the reference temperature at the end Z=L or $\bar{\zeta}$=1.

The temperature dependence of the modulus of elasticity for most engineering materials is given by:

$E(T_1) = E_1(1-\gamma T_1)$ (2)

Where E_1 is the value of the modulus of elasticity at the reference temperature, i.e., at T_1=0 along the Z direction. Taking the temperature at the end of the blade, i.e., at $\bar{\zeta}$=1 as reference temperature, the modulus variation becomes:

$E(\bar{\zeta}) = E_1[1-\alpha(1-\bar{\zeta})]$ (3)

Where the temperature gradient $\alpha = \gamma T_o$ $0 \le \alpha < 1$

FORMULATION OF 3D DEGENRATED SHELL ELEMENT

Following Huang [1988], the formulation of the finite element for three-dimensional degenerated curved shell is as follows:

It is assumed that the displacement of points at the midsurface are u'_o, v'_o and w'_o in the local coordinate directions x', y' and z', respectively. If the rotations θ_x and θ_y of the mid surface normal in the $x'-z'$ and $y'-z'$ plane are available then the following relations can be obtained at a typical material point p.

$$u' = u'_o + z'\theta_x$$
$$v' = v'_o + z'\theta_y \qquad (4)$$
$$w' = w'_o$$

If the displacements u'_o, v'_o and w'_o can be transformed to the global coordinate system as u_o, v_o and w_o then it is possible to write:

$$u_i = u_{oi} + x'_3(\theta'_{x1}\frac{\partial x_i}{\partial x'_1} + \theta'_{x2}\frac{\partial x_i}{\partial x'_2}) \qquad (5)$$

Strains are defined in terms of the local coordinate system of axes $x'_i(x'_1 = x', x'_2 = y', x'_3 = z')$, where x'_3 is perpendicular to the material surface layer (ζ=constant). Therefore, the strain components of interest are:

$$\varepsilon` = \begin{bmatrix} \varepsilon'_f \\ \varepsilon'_s \end{bmatrix} = \begin{bmatrix} \varepsilon'_x \\ \varepsilon'_y \\ \gamma'_{xy} \\ \gamma'_{xz} \\ \gamma'_{yz} \end{bmatrix} = \begin{bmatrix} \partial u'/\partial x' \\ \partial v'/\partial y' \\ \partial u'/\partial y' + \partial v'/\partial x' \\ \partial u'/\partial z' + \partial w'/\partial x' \\ \partial v'/\partial z' + \partial w'/\partial y' \end{bmatrix} \qquad (6)$$

Where ε'_f is the in plane strain vector defined in the local coordinates, ε'_s is a transverse shear strain vector, and u', v' and w' are the displacement components in the local system x'_i.

In the local Cartesian coordinate system with $x'-y'$ tangential to the shell midsurface, ε'_f can be divided into two parts, one associated with membrane, ε'_m and one associated with bending behavior, ε'_b so that:

$$\varepsilon'_f = \varepsilon'_m + \varepsilon'_b$$

Where:

$$\varepsilon'_m = \begin{bmatrix} \partial u'_o/\partial x' \\ \partial v'_o/\partial y' \\ \partial u'_o/\partial y' + \partial v'_o/\partial x' \end{bmatrix} \quad \text{and,} \quad \varepsilon'_b = \begin{bmatrix} z'\partial\theta'_x/\partial x' \\ z'\partial\theta'_y/\partial y' \\ z'(\partial\theta'_x/\partial y' + \partial\theta'_y/\partial x') \end{bmatrix} \qquad (7)$$

The global derivatives of the displacements u, v and w are transformed into local derivatives of the local displacements u', v' and w' by the standard operation:

$$\begin{bmatrix} \partial u'/\partial x' & \partial v'/\partial x' & \partial w'/\partial x' \\ \partial u'/\partial y' & \partial v'/\partial y' & \partial w'/\partial y' \\ \partial u'/\partial z' & \partial v'/\partial z' & \partial w'/\partial z' \end{bmatrix} = \theta^T \begin{bmatrix} \partial u/\partial x & \partial v/\partial x & \partial w/\partial x \\ \partial u/\partial y & \partial v/\partial y & \partial w/\partial y \\ \partial u/\partial z & \partial v/\partial z & \partial w/\partial z \end{bmatrix} \theta \qquad (8)$$

Where θ is the transformation matrix:

$$\theta = \begin{bmatrix} \partial x/\partial x' & \partial x/\partial y' & \partial x/\partial z' \\ \partial y/\partial x' & \partial y/\partial y' & \partial y/\partial z' \\ \partial z/\partial x' & \partial z/\partial y' & \partial z/\partial z' \end{bmatrix}$$

The global derivatives of the displacement u, v and w are obtained from the expression (9).
For a material, especially orthotropic, that possesses three mutually perpendicular axes of elastic symmetry, two of which (1,2) are tangential to the surface layer and the third (3) normal to it, then:

$$\varepsilon_1 = \frac{1}{E_1}(\sigma_1 - \upsilon_{12}\sigma_2 - \upsilon_{13}\sigma_3)$$

$$\varepsilon_2 = \frac{1}{E_2}(\sigma_2 - \upsilon_{21}\sigma_1 - \upsilon_{23}\sigma_3)$$

$$\varepsilon_3 = \frac{1}{E_3}(\sigma_3 - \upsilon_{31}\sigma_1 - \upsilon_{32}\sigma_2) \qquad (9)$$

$$\gamma_{12} = \tau_{12}/G_{12}$$

$$\gamma_{13} = \tau_{13}/G_{13}$$

$$\gamma_{23} = \tau_{23}/G_{23}$$

In which E_1, E_2 and E_3 are Young's moduli in the 1, 2, and 3 (material) directions, respectively, υ_{ij} is Poisson's ratio for transverse strain in the i direction when stressed in the j direction. G_{12}, G_{13} and G_{23} are the shear moduli in the 12, 13, and 23 planes, respectively. In view of the reciprocal relations $\upsilon_{ij}/E_i = \upsilon_{ji}/E_j$, and there being only nine independent elastic constants for an orthotropic elastic medium, assuming that a state of plane stress exists and that the change of shell thickness during deformation is negligible, then eq.(9) reduces, on use of standard relationships between the anisotropic material parameters, to,

$$\sigma_{1,2,3} = D\varepsilon_{1,2,3} \qquad (10)$$

Where,

$$\sigma_{1,2,3} = [\sigma_1, \sigma_2, \tau_{12}, \tau_{13}, \tau_{23}]^T$$

$$\varepsilon_{1,2,3} = [\varepsilon_1, \varepsilon_2, \gamma_{12}, \gamma_{13}, \gamma_{23}]^T \qquad (11)$$

$$D = \begin{bmatrix} D_1 & D_{12} & 0 & 0 & 0 \\ D_{21} & D_2 & 0 & 0 & 0 \\ 0 & 0 & D_3 & 0 & 0 \\ 0 & 0 & 0 & D_4 & 0 \\ 0 & 0 & 0 & 0 & D_5 \end{bmatrix} \qquad (12)$$

and,

$$D_1 = E_1 / \Delta$$
$$D_2 = E_2 / \Delta$$
$$D_{12} = E_2 \upsilon_{12} / \Delta$$
$$D_3 = G_{12} \tag{13}$$
$$D_4 = K_1 G_{13}$$
$$D_5 = K_2 G_{23}$$
$$\Delta = 1 - \upsilon_{12}\upsilon_{21}$$

The terms K_1 and K_2 are shear correction factors in the 13 and 23 planes, respectively that will be determined later.

In general, the principal axes of anisotropic 1,2 will not coincide with the reference axes x, y but will be rotated by some angle ω. Therefore, the constitutive relation, eq.(10), must be transformed, before use in determining the element stiffness matrix, as follows:

$$\sigma_{1,2,3} = \Omega_\sigma \sigma_{x,y,z}$$
$$\varepsilon_{1,2,3} = \Omega_\varepsilon \varepsilon_{x,y,z} \tag{14}$$

Where,

$$\sigma_{x,y,z} = \left[\sigma_x, \sigma_y, \tau_{xy}, \tau_{xz}, \tau_{yz}\right]^T$$
$$\varepsilon_{x,y,z} = \left[\varepsilon_x, \varepsilon_y, \gamma_{xy}, \gamma_{xz}, \gamma_{yz}\right]^T$$

It is convenient to write the constitutive equations in the partitioned form:

$$\sigma' = \begin{bmatrix} \sigma'_f \\ \sigma'_s \end{bmatrix} = \begin{bmatrix} \sigma'_x \\ \sigma'_y \\ \tau'_{xy} \\ \tau'_{xz} \\ \tau'_{yz} \end{bmatrix} = D' \begin{bmatrix} \varepsilon'_f \\ \varepsilon'_s \end{bmatrix} \tag{15}$$

Where $\sigma'_f(\varepsilon'_f)$ and $\sigma'_s(\varepsilon'_s)$ are the in-plane stresses (strains) and transverse shear stresses (strains) respectively, defined in the local coordinates and:

$$D' = \begin{bmatrix} D'_f & 0 \\ 0 & D'_s \end{bmatrix} \tag{16}$$

For an isotropic material:

$$D'_f = \begin{bmatrix} \lambda' + 2G & \lambda' & 0 \\ \lambda' & \lambda' + 2G & 0 \\ 0 & 0 & G \end{bmatrix}$$

$$D'_s = \begin{bmatrix} KG & 0 \\ 0 & KG \end{bmatrix}$$

Here K is a shear correction factor taken equal to (5/6) for a homogenous cross section. The term G is the shear modulus and λ' is the plane stress reduced $\lambda' = \upsilon E / (1 - \upsilon^2)$, E is the modulus of elasticity and υ is Poisson's ratio.

<u>The Total Potential Energy</u>

In the local coordinate system, the total potential energy for the degenerated shell is given as:

$$\Pi = \frac{1}{2}\int_v \varepsilon_f'^T D_f' \varepsilon_f' dv + \frac{1}{2}\int_v \varepsilon_s'^T D_s' \varepsilon_s' dv - W \qquad (17)$$

Where W is the potential energy of the applied loads.

Element Geometry

In the degenerated shell element, each node has five degrees of freedom, i.e., three translational displacements in the direction of the global axes and two rotations with respect to axes in the plane of the middle surface as shown in **Fig. (1)**. The Cartesian coordinate at any point of the shell can be uniquely given in terms of nodal coordinate of a point at the vector V_3^k can be expressed as,

$$\bar{x}_i^k = x_i^k + \frac{\zeta}{2} h V_{3i}^k \qquad (i=1,2,3) \qquad (18)$$

$$x_i = \sum_{k=1}^{n} N^k(\xi,\eta)\bar{x}_i^k$$

$$x_i = \sum_{k=1}^{n} N^k(\xi,\eta)x_i^k + \frac{\zeta}{2}\sum_{k=1}^{n} N^k(\xi,\eta)h^k V_{3i}^k \qquad (i=1,2,3) \; (19)$$

Alternatively, the global coordinates of pairs of points on the top and bottom surfaces at each node are usually input to define the element geometry. Thus,

$$x_i = \sum_{k=1}^{n} N^k(\xi,\eta)\left[\frac{1+\zeta}{2} x_{i,top}^k + \frac{1-\zeta}{2} x_{i,bottom}^k\right] \qquad (i=1,2,3) \qquad (20)$$

Where :

x_i =Cartesian coordinate of any point in the element, ($x_1 = x, x_2 = y, x_3 = z$)

x_i^k =Cartesian coordinate of any point k.

h^k =Thickness of shell in ζ direction at nodal point k.

V_{3i}^k = i_{th} Component of the unit normal vector to the middle surface.

$N^k(\xi,\eta)$=The two-dimensional interpolation function corresponding to node k

ζ =The distance from the middle surface.

Displacement Field

The displacements at any point in the shell element are defined by the three Cartesian components of the midsurface node displacement u_{oi}^k and two rotations of the nodal vector V_3^k about the orthogonal direction normal to it. According to Omprakash and Ramamurti, [1989], the displacements u_i^k along the thickness at each nodal point are,

$$u_i^k = u_{oi}^k + x_3'\left[\theta_{x_1'}^k\left(\frac{\partial x_l}{\partial x_1'}\right)^k + \theta_{x_2'}^k\left(\frac{\partial x_l}{\partial x_2'}\right)^k\right] \qquad (21)$$

$$\therefore u_i^k = u_{oi}^k + \frac{\zeta}{2}h^k\left(V_{1i}^k\alpha_1^k - V_{2i}^k\alpha_2^k\right)$$

Thus, the same expression as that is obtained as:

$$u_i = \sum_{k=1}^{n} N^k(\xi,\eta) u_i^k$$

$$u_i = \sum_{k=1}^{n} N^k(\xi,\eta) u_{oi}^k + \frac{\zeta}{2}\sum_{k=1}^{n} N^k(\xi,\eta) h^k \left(V_{1i}^k \alpha_1^k - V_{2i}^k \alpha_2^k\right) \quad (i=1,2,3) \qquad (22)$$

$$\therefore u_i = \sum_{k=1}^{n} \overline{N}^k(\xi,\eta,\zeta) d^k$$

and,

$$d^k = \left[u_{o1}^k \quad u_{o2}^k \quad u_{o3}^k \quad \alpha_1^k \quad \alpha_2^k\right]^T \qquad (23)$$

Where u_{oi}^k is the displacement of the k_{th} nodal point in the Cartesian coordinate, α_1^k and α_2^k are the rotations about V_2^k and V_1^k, respectively. It is noticed that,

$$\theta_{x_1'}^k = \alpha_1^k$$
$$\theta_{x_2'}^k = -\alpha_2^k \qquad (24)$$

Apparently, the displacement function assumed in eq.(22) is true only for small rotations.
It should be noted that in the implementation of the finite element method, V_3^k is not necessarily normal to the shell midsurface. Consequently, a certain approximation is introduced by the violation of the assumption of the straight 'normal'. According to Huang [1988], the strain components should be defined in terms of the local coordinate system in which the local derivatives of the displacement u', v' and w' are obtained from the global derivatives of the displacements u, v and w.
The global derivatives of the displacements u, v and w are given by,

$$\begin{bmatrix} \frac{\partial u}{\partial x} & \frac{\partial v}{\partial x} & \frac{\partial w}{\partial x} \\ \frac{\partial u}{\partial y} & \frac{\partial v}{\partial y} & \frac{\partial w}{\partial y} \\ \frac{\partial u}{\partial z} & \frac{\partial v}{\partial z} & \frac{\partial w}{\partial z} \end{bmatrix} = J^T \begin{bmatrix} \frac{\partial u}{\partial \xi} & \frac{\partial v}{\partial \xi} & \frac{\partial w}{\partial \xi} \\ \frac{\partial u}{\partial \eta} & \frac{\partial v}{\partial \eta} & \frac{\partial w}{\partial \eta} \\ \frac{\partial u}{\partial \zeta} & \frac{\partial v}{\partial \zeta} & \frac{\partial w}{\partial \zeta} \end{bmatrix} \qquad (25)$$

$$J = \begin{bmatrix} \frac{\partial x}{\partial \xi} & \frac{\partial y}{\partial \xi} & \frac{\partial z}{\partial \xi} \\ \frac{\partial x}{\partial \eta} & \frac{\partial y}{\partial \eta} & \frac{\partial z}{\partial \eta} \\ \frac{\partial x}{\partial \zeta} & \frac{\partial y}{\partial \zeta} & \frac{\partial z}{\partial \zeta} \end{bmatrix} \qquad (26)$$

In eq.(25) the displacement derivatives referred to the curvilinear coordinate are obtained from eq.(26). The strain-displacement matrix B, relating the strain components in the local system to the element nodal variables, can then be constructed as,

$$\varepsilon' = \sum_{k=1}^{n} B_i d_i \qquad (27)$$

Where ε' and d_i are defined in eq.(2) and eq.(23), respectively, and B is a matrix with five rows and a number of columns equal to the element nodal variables.
It is convenient to write eq.(27) in the partitioned from,

$$\begin{bmatrix} \varepsilon'_f \\ \varepsilon'_s \end{bmatrix} = \begin{bmatrix} \sum_{k=1}^{n} B_{fi} d_i \\ \sum_{k=1}^{n} B_{si} d_i \end{bmatrix} \quad (28)$$

in which ε'_f and ε'_s are the in plane strains, and the transverse shear strains defined by eq.(2).

Assumed that there is a zero stress in the direction perpendicular to five stress and strain components in the local system.

The total potential energy can be written as,

$$\Pi = \sum_e \Pi_e \quad (29)$$

Thus,

$$\Pi_e = \frac{1}{2} d_e^T \left[\int_{ve} B^T D B dv \right] d_e - W$$

$$\Pi_e = \frac{1}{2} d_e^T \left[\int_{ve} B_f^T D_f B_f dv \right] d_e + \frac{1}{2} d_e^T \left[\int_{ve} B_s^T D_s B_s dv \right] d_e - W \quad (30)$$

Where the elasticity matrix D is divided into a bending part D_f and shear part D_s. Upon finite element discretization and subsequent minimization of π with respect to the nodal variable di the following equation are obtained,

$$K_{ij} d_j = f_i \quad (31)$$

in which the stiffness matrix K_{ij} linking nodes i and j has the following typical contributions emanating from the in-plane and transverse shear strain energy terms respectively,

$$K_{f.ij}^e = \int_{ve} B_{fi}^T D_f B_{fi} dv$$

$$K_{s.ij}^e = \int_{ve} B_{si}^T D_s B_{si} dv \quad (32)$$

Where a 2-point integration rule through the shell thickness and a full integration rule in the $\xi - \eta$ surface should be used and,

$$dv = dx'dy'dz' = |J| d\xi d\eta d\zeta$$

Where $|J|$ is the determinant of the Jacobian matrix.

Dynamic Equilibrium Equations

The semi discrete form of the dynamic equilibrium equations is obtained using the principle of virtual work which states that for any arbitrary kinematically consistent set of displacements, the virtual work done must equal that done by the external forces irrespective of the material behaviour, i.e.:

$$\int_v (\delta_\varepsilon)^T \sigma dv = \int_v (\delta_u)^T t ds + \int_v (\delta_u)^T (b - \rho \ddot{u} - c \dot{u}) dv \quad (33)$$

Where δ_u is a vector of virtual displacements, δ_ε is the vector of associated virtual strains and σ is the vector of stresses referred to the local coordinates. The term t is a vector of surface traction acting on the portion δ_t of the boundary δ. The vectors $b, \rho\ddot{u}$ and $c\dot{u}$ are the body, inertial and damping forces, respectively. The symbol (.) denotes differentiation with respect to time. ρ is the mass density and c is the damping parameter.

For a finite element representation of an isoparametric 'degenerated' shell element the displacements, velocities and accelerations $u, \dot{u}, \ddot{u}$ and their virtual counterparts can be defined in terms of the nodal variables $d, \dot{d}$ and $\ddot{d}$ by the expressions,

$$u = \sum_{i=1}^{m} \overline{N}_i(\xi,\eta,\zeta) d_i = \overline{N} d, \qquad \delta u = \overline{N}\delta d$$

$$\dot{u} = \sum_{i=1}^{m} \overline{N}_i(\xi,\eta,\zeta) \dot{d}_i = \overline{N}\dot{d} \qquad (34)$$

$$\ddot{u} = \sum_{i=1}^{m} \overline{N}_i(\xi,\eta,\zeta) \ddot{d}_i = \overline{N}\ddot{d}$$

Where $\overline{N}_i(\xi,\eta,\zeta)$ is the matrix of shape function.

With the standard strain matrix B we may relate the virtual strain vector to the nodal variables as,

$$\delta\varepsilon = \sum_{i=1}^{m} B_i \delta d_i = B\delta d \qquad (35)$$

Upon substitution of eq.(33) and eq.(34) into eq.(32),

$$\delta d^T \left[M\ddot{d} + c\dot{d} + p(d)\right] = \delta d^T f \qquad (36)$$

is obtained, in which the mass matrix M, the damping matrix C, the internal restoring force vector p(d) and the external applied load vector f have the following element contributions,

$$M_e = \int_{ve} \rho \overline{N}^T \overline{N} dv\ ; \quad C_e = \int_{ve} C\overline{N}^T \overline{N} dv; \quad P_e = \int_{ve} B^T \sigma dv; \quad f_e = \int_{se} \overline{N}^T t ds + \int_{ve} \overline{N}^T b dv \qquad (37)$$

Where s_e and v_e denote the surface and volume, respectively, of the element under consideration.

Since the virtual displacements δd may be arbitrary, eq. (36) may be written as,

$$M\ddot{d} + C\dot{d} + P(d) = f \qquad (38)$$

For linear elastic situations, the stresses σ are related to the strains ε as follows,

$$\sigma = D\varepsilon = DBd$$

Therefore, the internal restoring forces P(d) can be rewritten as,

$$P(d) = Kd$$

Where,

$$K = \sum_e K_e = \sum_e \int_{ve} B^T DB dv \qquad (39)$$

In which K_e is the contribution to the structural stiffness matrix K from a typical element e.

Modeling of Mass Matrix

Consistent mass matrix, M_e, in eq.(37) represents a consistent mass matrix. The sub matrix of the element mass matrix linking nodes i and j can be expressed as,

$$M_{e.i,j} = \int_{ve} \overline{N}_i \rho \overline{N}_j dv \qquad (40)$$

Which does not lead to a diagonal mass matrix, when the adopted shape functions $\overline{N}$ are identical to those used in the evaluation of the element stiffness matrix.

For a typical node i, the diagonal mass term m_{ii} of the *lumped mass matrix* associated with (u,v,w) can be evaluated by the expression,

$$m_{ii} = \omega_i \int_{ve} \rho dv \qquad (41)$$

Where ω_i is a multiplier and ρ is the density of the plate or shell element. The diagonal rotary inertia I_{ii1} and I_{ii2} associated with vector V_1 and V_2 are also considered in this work, because their importance has been proven for thick plates. The rotary inertia are given as,

$$I_{ii1} = I_{ii2} = \omega_i \int_{ve} \rho z'^2 dv \tag{42}$$

$$\text{and, } \omega_i = \frac{\int_{ve} \rho N_i N_i dv}{\sum_{k=1}^{n} \int_{ve} \rho N_k N_k dv} \tag{43}$$

Where n is the number of nodes for each element. For the layered element,

$$I_{ii1} = I_{ii2} = \omega_i \int_{sm} \sum_{J} \rho_j h_j \left(z'^2 + \frac{h_j^2}{12} \right) dx'dy' \tag{44}$$

Where h_j represents the thickness of the jth layer and in its evaluation, summation is made over the number of layers. The term z'_j is the distance of the layer middle surface sm. The rotary inertia for a non-layered element is approximately equal to,

$$I_{ii1} = I_{ii2} = m_{ii} \frac{h_i^2}{4} \tag{45}$$

Eq.(45) can be thought of as a resultant of the lumped mass $m_{ii}/2$ concentrated at each end of the vector V'_3 about the axis normal to it. The lumped mass matrix for node i of the shell can be written as,

$$M_i = \begin{bmatrix} m_{ii} & 0 & 0 & 0 & 0 \\ 0 & m_{ii} & 0 & 0 & 0 \\ 0 & 0 & m_{ii} & 0 & 0 \\ 0 & 0 & 0 & I_{ii1} & 0 \\ 0 & 0 & 0 & 0 & I_{ii2} \end{bmatrix} \tag{46}$$

SOLUTION OF EIGNVALUE PROBLEM

To solve eq.(38), Newmark's algorithm together with the Hughes and Liu predictor-corrector scheme is adopted. The parameters γ and β are used to control the stability and accuracy of the solution. In the present work a conditionally stable time stepping scheme is adopted with $\gamma = 0.5$ and $\beta = 0.25$.

For free vibration motion the external force f is equal to zero and if the displacements are assumed to be harmonics as:

$$d = Xe^{i\omega t} \tag{47}$$

then eq.(41) gives the following free vibration equation,

$$(K - \omega^2 M)X = 0 \tag{48}$$

which is called a linear algebraic eignvalue problem.

Generally, there are two methods for solving eigenvalue problem. The transformation methods, such as Jacobi, and Householder schemes are preferable when all the eignvalues and eignvectors are required. The iterative methods, such as the power method, are preferable when few eignvalue and eignvector are required. Since the designer is interested in finding the first lower natural frequencies of the structures, the iterative method in solving the eignvalue problem is used.

The method of *Rayleigh-Ritz subspace iteration* can be used to find the lowest eignvalues and the associated eignvectors of the general eignvalues problem, Bathe [1982]. It is very effective in finding the first few eignvalues of the problem whose stiffness K and mass M matrices have large bandwidth.

RESULTS AND DISCUSSIONS

Results and discussions of the previously described analysis of a rotating blade are presented here. The reliability of the theoretical work and computer programs output are investigated by making comparisons of the present results with some known experimental and theoretical solutions.

Convergence Test

To verify the convergence, stresses and deformations are computed for different mesh sizes. They are used for a certain blade geometry dimensions in order to design a suitable mesh size to be used during the analysis. The mesh sizes are shown in **Fig.(2)**. **Fig.(3)** shows the variation of v-deflection with the degree of freedom. In this figure, the deflection values are those established after 135 degree-of-freedom, DOF. **Fig. (4)**, **(5)**, and **(6)** show the variations of xx-stresses, yy-stresses and xy-shear stresses, respectively, with the degree of freedom. In all figures, the stresses in all directions are shown and their values stabilized after 175 DOF. Hence, it is preferable that the satisfactory mesh size, for the current analysis, consists of three elements across the length and two elements across the width.

Verification Test

The results of the current work, presented in **Tables (1), (2), (3)**, and **(4)**, are compared with that of Bathe [1982]. **Table (1)** shows the maximum tip deflections, where the pre-twist angle is 0^o. The present results are related with those results by Abbas and H. Irretier, [1989]. **Table (2)** also demonstrates the same comparison in **Table (1)** but at pre-twist angle equal to 15^o. In both tables the maximum error does not exceed 0.42%. **Table (3)** shows the maximum radial stresses when the pre-twist angle is 0^o. The differences between the current results and the results of Bathe [1982] are larger than the deflection results. **Table (4)** indicates the same correspondence in **Table (3)** but at pre-twist angle equal to 15^o. In both tables the maximum error e does not exceed 7.8%.

Thermal Effects

In order to investigate the thermal effects, three values [0.02, 0.06, and 0.10] of thermal gradient are used. **Fig.(7)** exhibits the variation of v-deflections with thermal gradient at different values of pre-twist angles. It is observed that when thermal gradient increases, v-deflection increases too. **Fig. (8), (9)**, and **(10)** display the variations of xx-stresses, yy-stresses, and xy-shear stresses at different values of pre-twist angles. In all figures, it is shown that when thermal gradient increased, the stresses in all directions decrease. **Fig. (11)** shows the variation of v-deflections with thermal gradient at different values of skew angle. This figure shows that when thermal gradient increases, the v-deflections increase. **Fig. (12), (13)**, and **(14)** demonstrate the variations of xx-stresses, yy-stresses, and xy-shear stresses with thermal gradient at different values of skew angle. In all figures, it is seen that when thermal gradient increases, the stresses in all directions increase too. Generally, thermal gradient causes large deformations in the blade. Hence, the thermal gradient along the blade must be lowered.

VIBRATION ANALYSIS

The vibration characteristics of blade are studied since the evaluation of natural frequencies, and mode shapes is important in order to avoid resonance.

Verification Test

In this test, the current results are compared with the experimental and theoretical results in Bathe, [1982]. **Table (5)** compares the current results with experimental and theoretical results in Bathe, [1982] and the values of percentage error with experimental and theoretical results. In this table, it is seen that the percentage errors between the current results and experimental results are less than the percentage errors between the experimental results and the numerical integration results of Bathe, [1982].

Thermal Effects

In order to study the effect of thermal gradient on natural frequencies, three values of thermal gradient [0.1, 0.06, and 0.02] were selected. **Fig. (15)** shows the variation of natural frequency with thermal gradient at different pre-twist angles. It is seen that when the thermal gradient increases the natural frequency decreases. **Fig. (16)** shows the variation of natural frequency with thermal gradient at different skew angles. It is observed that when thermal gradient increases, the natural frequency decreases too. For this reason, thermal gradient effects represent very important parameters in the design of blades because it reduces the natural frequencies and that causes failure to the blade under relatively low speed. Consequently, few designers take this effect as a major parameter in the design as Fauconneau and Marangont, [1970] and Tomar and Jain, [1984], it is believed thermal gradient is one of the important reasons for failure of the turbine blades and any part working under high temperature. Thus, the thermal gradient is kept as small along the blade, as possible.

CONCLUSIONS

The conclusions obtained from the present works can be summarized as follows:

1- Thermal gradient reduces the stresses but raises the deformations in blade.
2- Thermal gradient minimizes the natural frequency of the blade and it represents a very important parameters in the design of blade working at higher temperatures. Thermal gradient represents one of the important parameters that cause failure of the blade, which works at high temperatures and speeds.

Table (1) Effect of radius of rotation on tip v-deflections (pre-twist angle $=0^{o}$)

Ratio	Present	Ref. [12]	Error
0	20.98	20.91	0.33%
1	28.83	28.73	0.34%
2	36.68	36.74	0.16%
3	44.54	44.36	0.40%
4	52.39	52.17	0.42%
5	60.24	59.99	0.41%

Table (2) Effect of radius of rotation on tip v- deflections (pre-twist angle $=15^{o}$)

Ratio	Present	Ref. [12]	Error
0	20.99	20.94	0.23%
1	28.95	28.88	0.24%
2	36.91	36.82	0.24%
3	44.87	44.76	0.24%
4	52.83	52.71	0.22%
5	60.79	60.65	0.23%

Table (3) Effect of radius of rotation on yy-stresses (pre-twist angle $=0^{o}$)

Ratio	Present	Ref. [12]	Error
0	8.26	8.81	6.2%
1	12.19	13.05	6.5%
2	16.13	17.29	6.7%
3	20.06	21.54	6.8%
4	24.01	25.78	6.8%
5	27.93	30.02	6.9%

Table (4) Effect of radius of rotation on yy-stresses (pre-twist angle $=15^{o}$)

Ratio	Present	Ref. [12]	Error
0	8.3	8.83	5.0%
1	12.5	13.43	6.9%
2	16.7	18.02	7.3%
3	20.9	22.62	7.6%
4	25.1	27.21	7.7%
5	29.3	31.81	7.8%

Length/Width =4, Density =7850 kg/m^3, Thickness/Width =0.12, Skew angle =90°, Width =0.1 m
Speed of rotation =2500 r.p.m., Ratio =Radius/length Young's modulus =207 MN/m^2

Note

v-deflection and yy-stresses put in dimensionless, where:

v-deflection $= v_{yy(\max.)} \big/ \left(\rho\Omega^2 b^3/E\right)$ yy-stresses $= \sigma_{yy(\max.)} \big/ \left(\rho\Omega^2 b^2\right)$

Table (5) Values of first natural frequency of blades[Hz]

Length	Experimental*	Theoretical**	Present	Error with Exp.	Error with theor.
0.3175	88.90	91.30	91.46	2.87%	0.17%
0.1588	345.30	365.10	364.97	5.69%	0.03%
0.1058	747.80	821.50	819.42	9.57%	0.25%
0.0794	1300.00	1460.50	1447.49	11.34%	0.89%
0.0635	1968.30	2282.20	2247.66	14.19%	1.51%
0.0529	2736.80	3286.30	3211.11	17.33%	2.28%
0.0455	3594.70	4473.10	4297.95	19.56%	3.91%
0.0397	4550.00	5842.40	5579.36	22.63%	4.50%
0.0353	5513.50	7394.30	6966.67	26.35%	5.78%
0.0318	6731.80	9128.70	8465.62	25.75%	7.26%

Width of blade =0.025 m, Thickness of blade =0.011 m, Poisson's ratio =0.3, Mass density =7850 Kg/m^3
Modulus of elasticity =208 GN/m^2

* Bathe, [1982]

** Bathe, [1982]

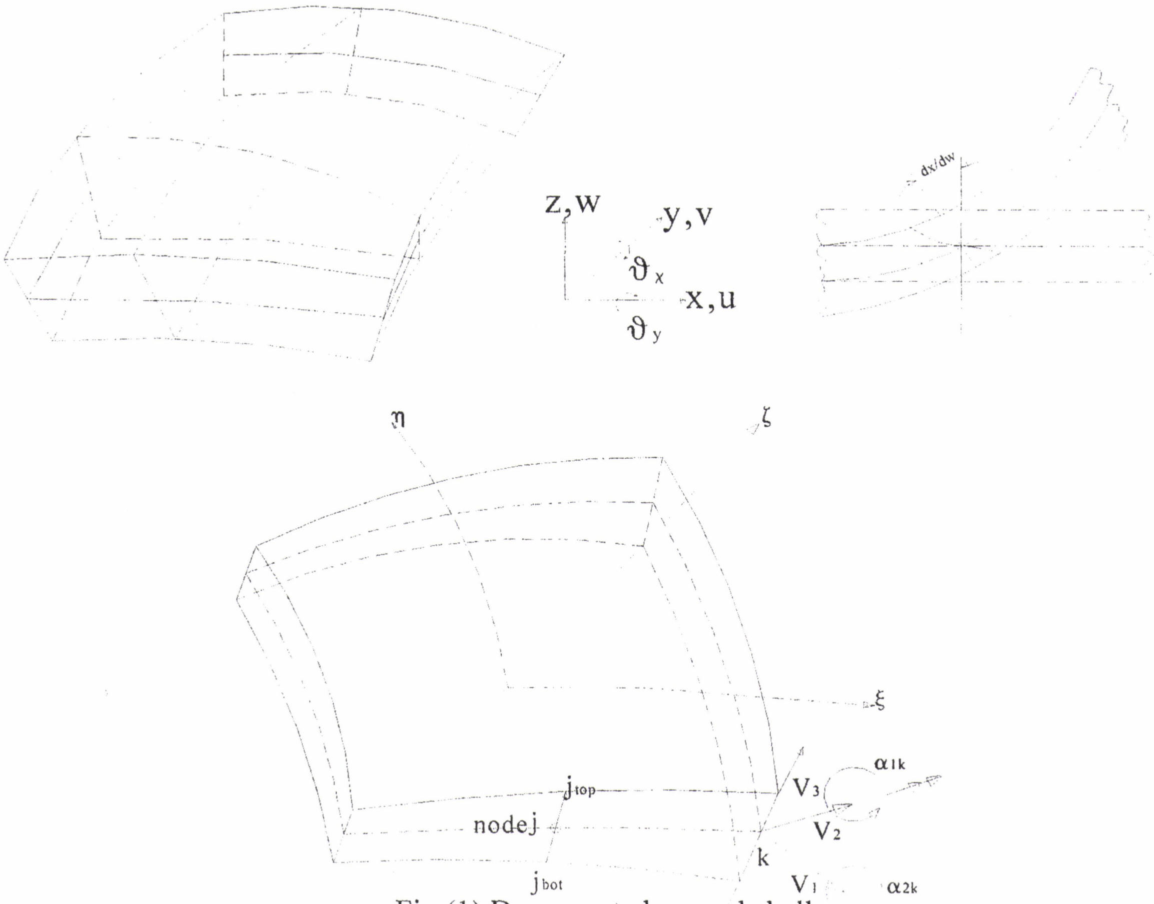

Fig (1) Degenerated curved shell

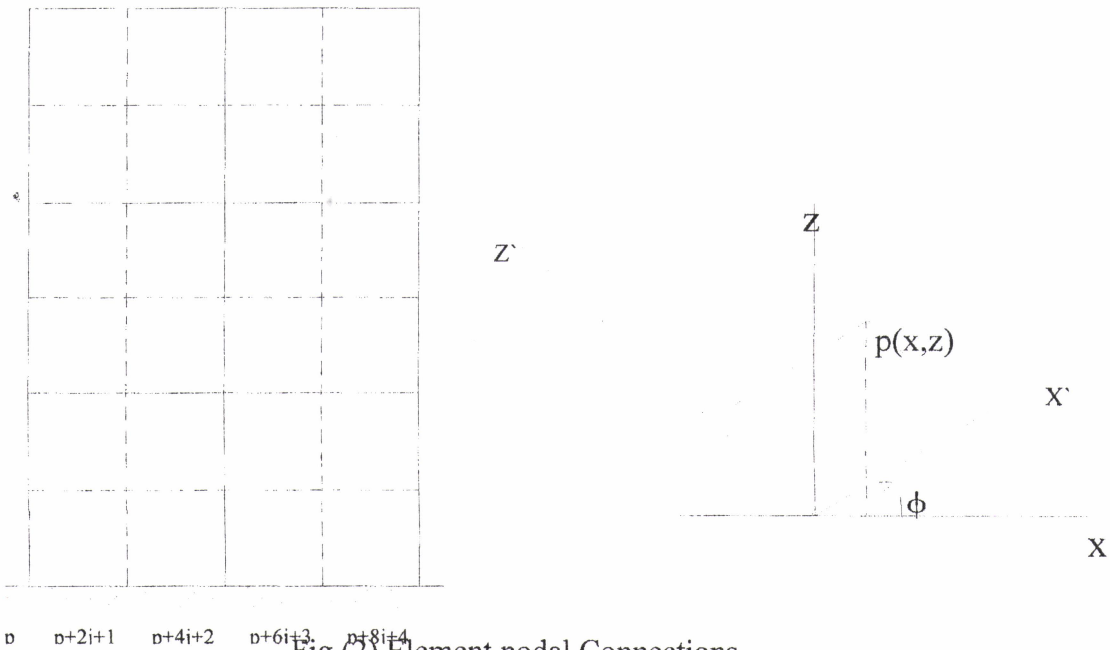

Fig (2) Element nodal Connections

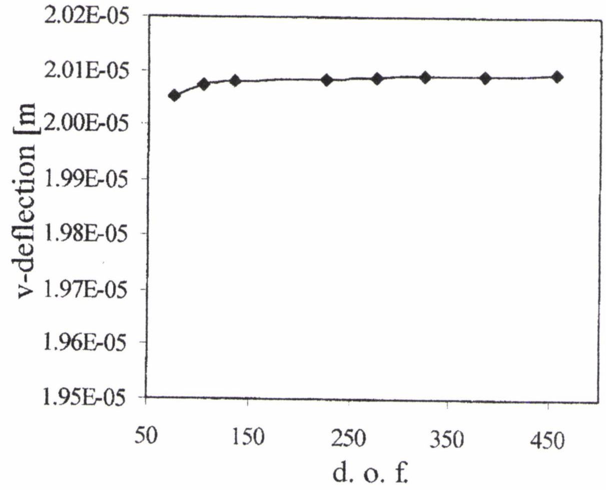

Fig (3) Variation of v-deflections with degree of freedom

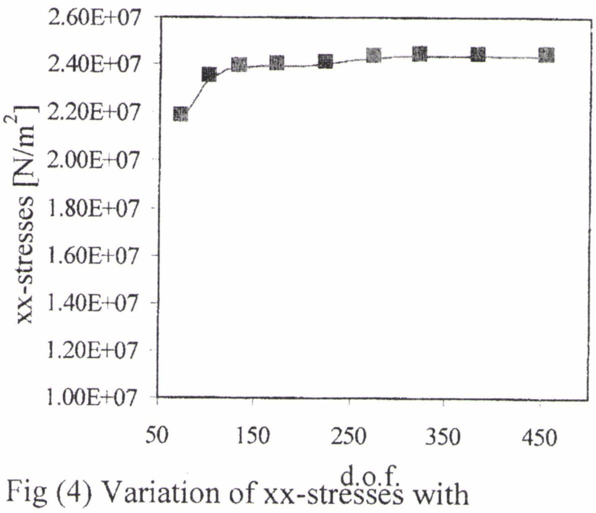

Fig (4) Variation of xx-stresses with degree of freedom

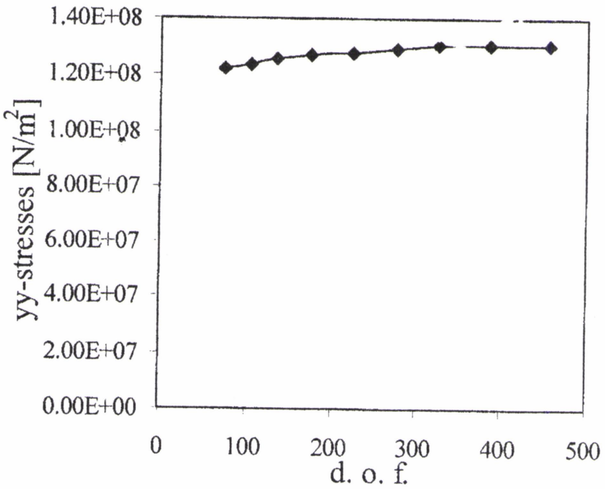

Fig (5) Variation of yy-stresses with degree of freedom

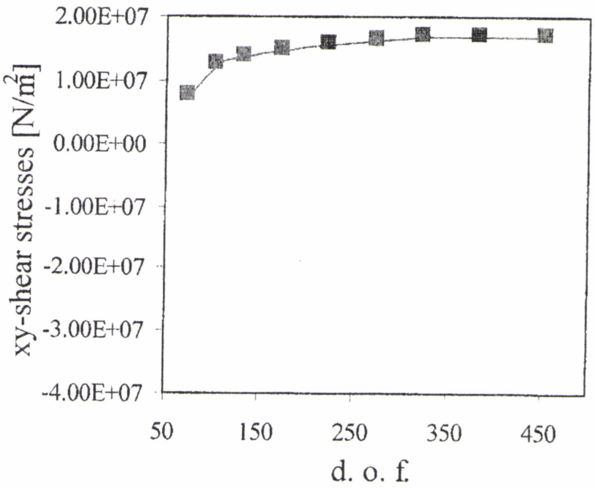

Fig (6) Variation of xy-shear stresses with degree of freedom

Skew angle $=0^{o}$

Pre-twist angle $=0^{o}$

Density =7850 kg/m^3

Young's modulus =207 GN/m^2

Poisson's ratio =0.25

Speed of rotation =10000 r.p.m.

Radius of blade =0.18034 m

Length of blade =0.06604 m

Width of blade =0.031475 m

Thickness of blade =0.003175 m

(Low Carbon Steel)

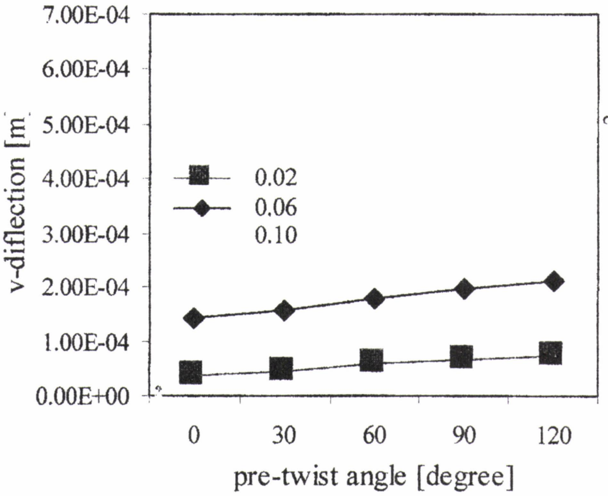

Fig (7) Variation of v-deflections with thermal gradient

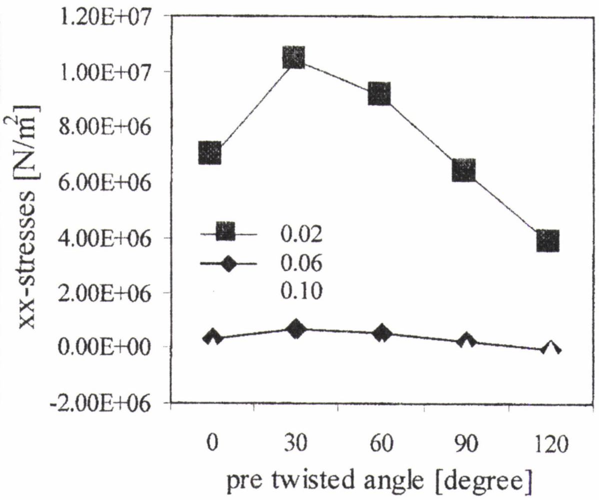

Fig (8) Variation of xx-stresses with thermal gradient

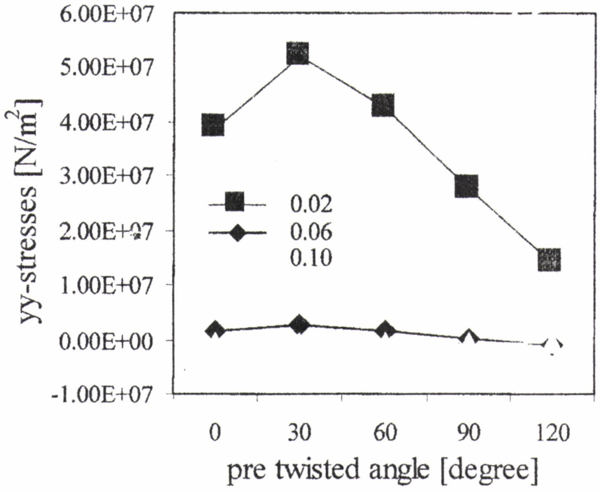

Fig (9) Variation of yy-stresses with thermal gradient

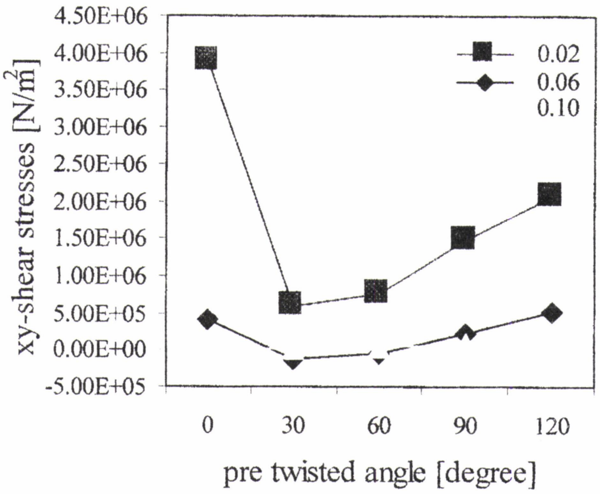

Fig (10) Variation of xy-shear stresses with thermal gradient

Pre-twist angle $=0^{o}$

Density $=7850$ kg/m^3

Young's modulus $=207$ GN/m^2

Poisson's ratio $=0.25$

Speed of rotation =10000 r.p.m.

Radius of blade =0.18034 m

Length of blade =0.06604 m

Width of blade =0.031475 m

Thickness of blade =0.003175 m

(Low Carbon Steel)

Skew angle $=0^{o}$

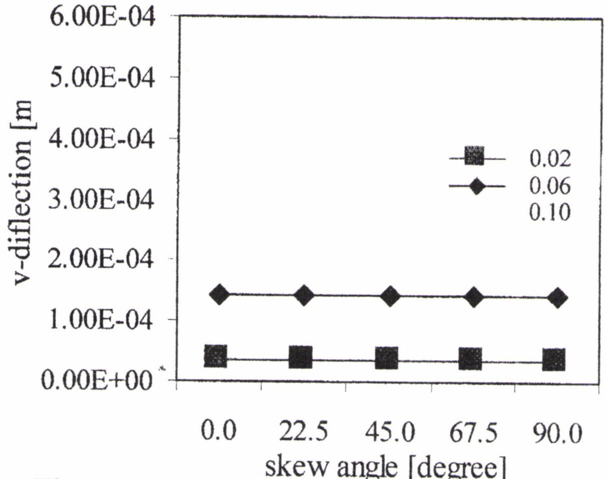

Fig (11) Variation of v-deflections with thermal gradient

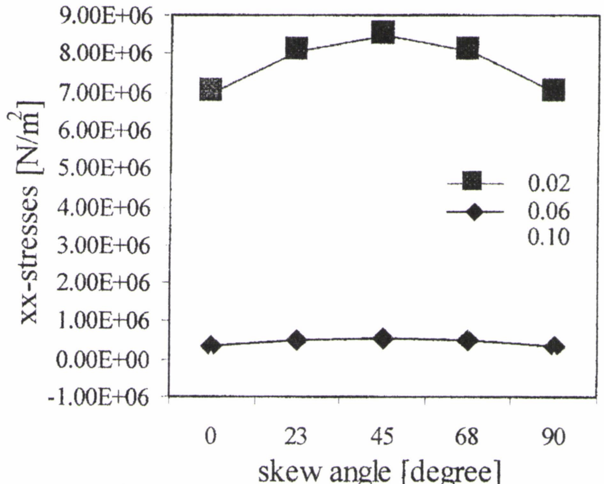

Fig (12) Variation of xx-stresses with thermal gradient

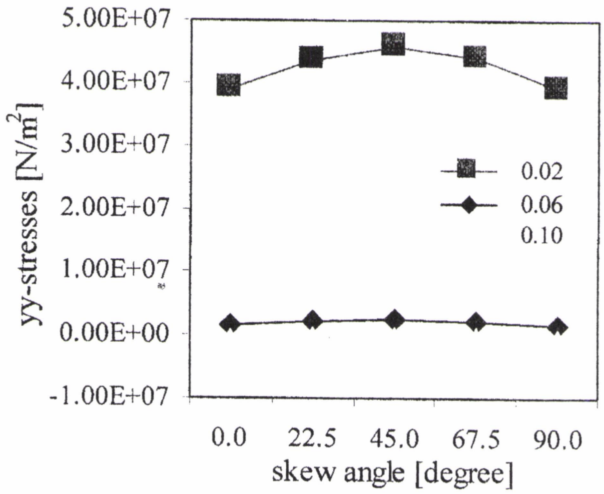

Fig. (13) Variation of yy-stresses with thermal gradient

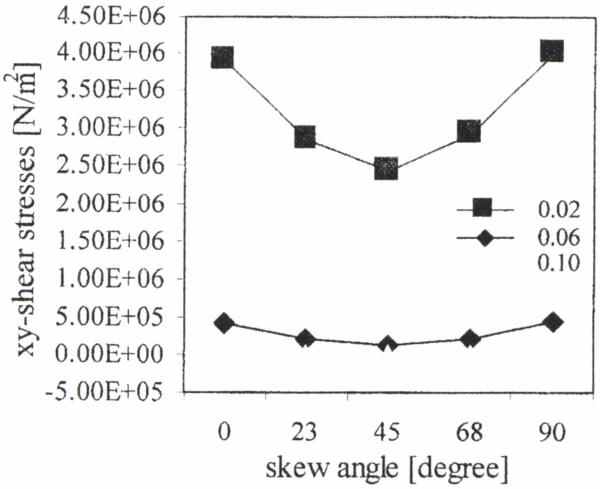

Fig. (14) Variation of xy-shear stresses with thermal gradient

Skew angle $=0^{o}$

Pre-twist angle $=0^{o}$

Density =7850 kg/m^3

Young's modulus =207 GN/m^2

Poisson's ratio =0.25

Speed of rotation =10000 r.p.m.

Radius of blade =0.18034 m

Length of blade =0.06604 m

Width of blade =0.031475 m

Thickness of blade =0.003175 m

(Low Carbon Steel)

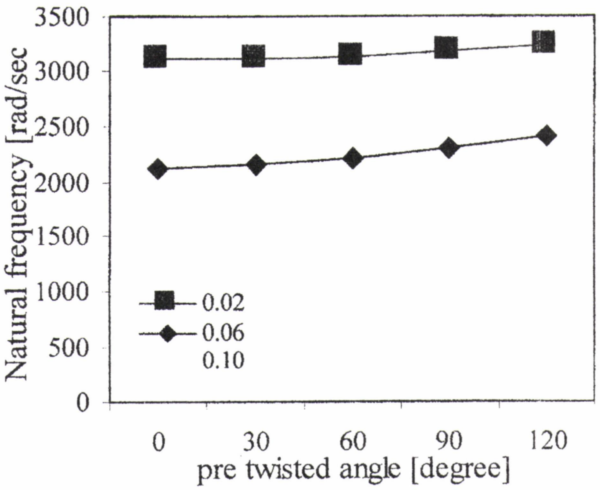

Fig (15) Variation of natural frequency with thermal gradient

Density = 7850 Kg/m3, E=207 MN/m^2, ν=0.25

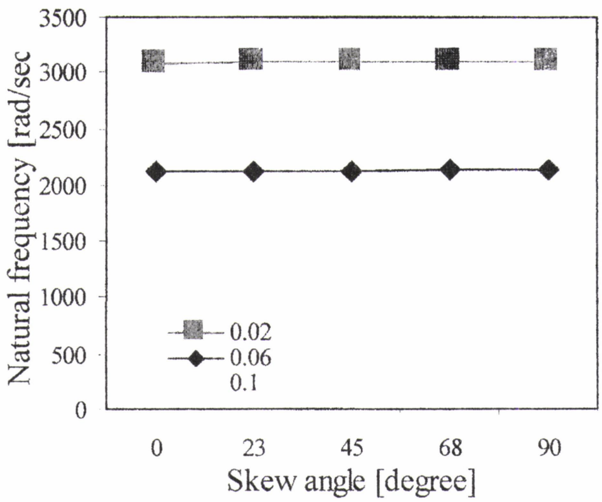

Fig (16) Variation of natural frequency with thermal gradient

Radius of blade =0.18034 m

Length of blade =0.06604 m $_{m^2}$

Thickness of blade =0.03175 m

Width of blade =0.031475 m

REFERENCE

Abbas B. A. H. and Irretier H., (1989), 'Experimental and Theoretical Investigations of the Effect of Root Flexibility on the Vibration Characteristics Beams', J. of Sound and Vibrations, Vol. 130, No. 3, pp.353-362,.

Bathe K. J.;(1982), 'Finite Element Procedure in Engineering Analysis' Prentice Hill.

Carnegie W., (1957), 'Static Bending of Pre-twisted Cantilever Blading', J. of Proceedings of the Institute of Mechanical Engineering, Vol. 171, pp.873-890.

Fauconneau G. and Marangont R.D., (1970), 'Effect of a Thermal Gradient on the Natural Frequencies of a Rectangular Plate', Int. J. of Mechanical Science, Vol. 12, pp.113-122,.

Huang H. C., 1988, 'Static and Dynamic Analysis of Plates and Shells', Springer-Verlag, First Edition,.

Omprakash V. and Ramamurti V., (1989), 'Dynamic Stress Analysis of Rotating Turbomachinery Bladed Disk Systems', J. of Computers and Structures, Vol. 32, No. 2, pp.477-488

Sisto F. and Chang A. T., (1984), 'A Finite Element for Vibration Analysis of Twisted Blades Based on Beam Theory', J. of AIAA, Vol. 22, No.11, pp.1646-1651,.

Tomar J. S. and Jain R., (1984), 'Effect of Thermal Gradient on Frequencies of a Wedge Shaped Rotating Beams', J. of AIAA, Vol. 22, No. 6, pp.848-850.

Tomar J. S. and Jain R., (1984), 'Thermal Effect on Frequencies of Coupled Vibrations of a Rotating Beam of Linearly Varying Semi Circular Cross Section', J. of Sound and Vibrations, Vol. 95, No. 1, pp.1-7.

Tomar J. S. and Jain R., (1985), 'Thermal Effect on Frequencies of Coupled Vibrations of Pre Twisted Rotating Beams', J. of AIAA, Vol. 23, No. 8, pp.1293-1296,.

NOTATION

B	Strain-displacement matrix
B_f	In-plane strain-displacement matrix
B_s	Bending strain-displacement
B_m	Transverse shear strain-displacement matrix
$\overline{B}_f$	Assumed in-plane strain-displacement matrix
$\overline{B}_s$	Assumed transverse shear strain-displacement matrix
D	Elasticity matrix, *N/mm²*
e_m	Membrane strain tensor in the orthogonal curvilinear coordinate system
$\overline{e}_m$	Assumed membrane strain tensor in the orthogonal curvilinear coordinate.
E	Young's modulus, *N/mm²*
J	Jacobian matrix
$\lvert J \rvert$	Determinant of the Jacobian matrix
K	Stiffness matrix, *N/mm*
K_f	In-plane stiffness matrix, *N/mm*
K_b	Bending stiffness matrix, *N/mm*
K_m	Membrane stiffness matrix, *N/mm*
K_s	Transverse shear stiffness matrix, *N/mm*
M_x, M_y, M_{xy}	Generalized stress components, *N.m/mm²*
N	Shape function
N_x, N_y, N_{xy}	Generalized stress components (in-plane forces), *N/mm*
Q_x, Q_y	Generalized stress components (shear forces), *N/mm*
T_1	Temperature excess above the reference temperature at any point at a distance $\overline{\zeta}=Z/L$
T_o	Temperature excess above the reference temperature at the end $Z=L$ or $\overline{\zeta}=1$.
$u_i(u, v, w)$	Displacement components, *mm*
W	Potential energy of loads, *N.m*
Z	Z-direction coordinate.
$\gamma_{xz}, \gamma_{xy}, \ldots$	Transverse shear strain components in the Cartesian coordinate system
$\gamma_{\eta\zeta}, \gamma_{\eta\xi}, \ldots$	Transverse shear strain components in the natural coordinate system
$\overline{\gamma}_{\eta\zeta}, \overline{\gamma}_{\eta\xi}, \ldots$	Assumed transverse shear strain components in the natural coordinate system
ε	Linear strain tensor
ε_f	In-plane strain tensor

ε_b	Bending strain tensor
ε_m	Membrane strain tensor
ε_s	Transverse shear strain tensor
$\overline{\varepsilon}_s$	Assumed transverse shear strain tensor
θ_x, θ_y	Rotations
ν	Poisson's ratio
π	Total potential energy
σ	Stress tensor, N/mm^2